

Dramatic extension of the high-order harmonic cutoff by using a long-wavelength driving field

Bing Shan* and Zenghu Chang*[†]

Center for Ultrafast Optical Science, University of Michigan, Ann Arbor, Michigan 48109

(Received 21 August 2001; published 14 December 2001)

We present an experimental demonstration of extending the high-order harmonic cutoff photon energy more than a factor of 2 when the driving-field wavelength is changed from 0.8 to 1.51 μm with an optical parametric amplifier. With argon gas, the cutoff has been extended from 64 to 160 eV. We predict that coherent keV x rays can be generated by exciting helium gas with the long-wavelength driving pulses. Experiments on xenon gas with several pump wavelengths also showed the dramatic cutoff extension, as well as full tunability of the generated XUV wavelengths.

DOI: 10.1103/PhysRevA.65.011804

PACS number(s): 42.65.Ky, 32.80.Rm

High-order harmonic generation (HHG) provides a unique way to produce coherent ultrafast soft x rays [1,2] and can be used in many applications such as ultrafast spectroscopy and microscopy [3,4]. While the highest photon energy ever produced is ~ 0.5 keV [5,6], great effort has been devoted to extend HHG into the keV x-ray regime, which will enable femtosecond time-resolved x-ray experiments to be performed by measuring x-ray diffraction from solids [7]. For spectroscopy applications, it is highly desirable to find a technique that can easily tune the x-ray wavelength to cover the range between adjacent orders. In this paper, we report that high-order harmonic generation pumped by an intense optical parametric amplifier is a promising way for developing an ultrafast, tunable, keV x-ray source.

Several methods have been proposed to extend the cutoff of high-order harmonic generation, for example, HHG from ions [8,9] or from core electrons [10], which are yet to be confirmed by experiments. In the tunneling regime, the dependence of cutoff photon energy on laser and atomic parameters is described explicitly as [5,11],

$$h\nu_{\text{cutoff}} = I_p + \left[\frac{0.5I_p^{3+a}\lambda^2}{\ln \frac{0.86\Delta t 3^{2n^*-1} G_{lm} C_{n^*l^*}^2 I_p}{-\ln(1-p)}} \right]^2, \quad (1)$$

where I_p is the ionization potential, Δt and λ are the duration and the wavelength of the laser pulse, respectively. $G_{lm} = (2l+1)(l+|m|)!/6^{|m|}|m|!(l-|m|)!$, and $C_{n^*l^*}^2 = 2^{2n^*}/n^*\Gamma(n^*+l^*+1)\Gamma(n^*-l^*)$. l and m are the orbital and magnetic quantum number. n^* is the effective principal quantum number, $l^* = l - n^*$ [12]. $p = 98\%$ is the ionization probability at the peak of the pulse. $a = 0.5$ is a correction of the analytical approximation. The results calculated with this formula agree well with the experimental results obtained by an 0.8- μm laser interacting with various atomic species.

Previously, extension of the cutoff photon energy has been successfully achieved by interacting atoms with ul-

trashort driving pulses, as indicated by Eq. (1). Pulses as short as 5–7 fs have been employed [4] and 0.5-keV x-ray emission was successfully generated. However, since such pulses are already approaching the one optical cycle, it is very hard to push the cutoff significantly by reducing the laser pulse further. According to Eq. (1), the cutoff photon energy strongly depends on the ionization potential, in fact, the record cutoff was achieved with helium, which has the largest ionization potential among all atoms. Ions can give even larger ionization potential, which offers another possibility to significantly extend the cutoff as shown by several simulations [8,9].

Another significant parameter in Eq. (1) is the wavelength of the driving pulse. Numerical simulations have been done on the dependence of cutoff on a driving-field wavelength with a 1053-nm laser and its second harmonic (526 nm) [13]. They found that the cutoff photon energy of HHG can be described by $E_{\text{max}} = I_p + 3U_p$, where U_p is the ponderomotive energy. It is clear in Eq. (1) that the cutoff photon energy for a given atomic state is proportional to the square of the wavelength. Figure 1 shows the calculation results of the relationship between the single-atom cutoff with the driving-field wavelength. The figure shows that by changing the driving-field wavelength from 0.8 to 1.6 μm , the cutoff of helium is extended from ~ 0.5 to 2 keV. This can be understood easily with the semiclassical three-step model [14,15]. First, the bound electrons of atoms tunnel through the Cou-

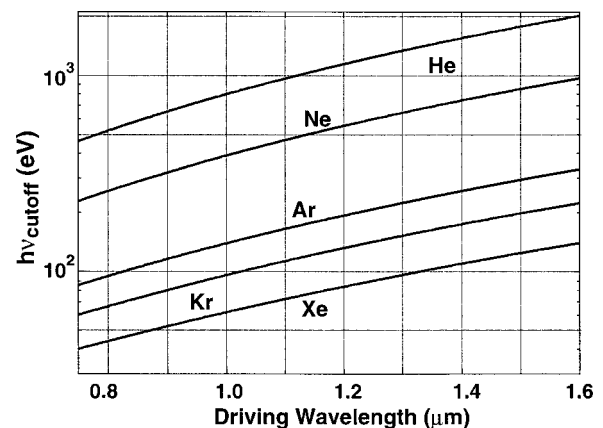


FIG. 1. Calculated relationship between single-atom HHG cutoff photon energy and the driving wavelength.

*Present address: Department of Physics, 116 Cardwell Hall, Kansas State University, Manhattan, KS 66506.

[†]Email address: chang@phys.ksu.edu

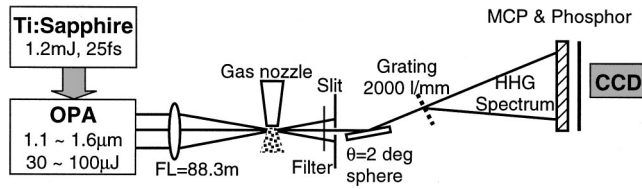


FIG. 2. Experimental setup for generating HHG with long-wavelength pump.

lomb barrier suppressed by the light field, then the free electrons move in the light field. When the light field reverses direction, some electrons move back towards their parent ions and are accelerated by the light field. Finally, when the electrons meet the parent ions, a portion of them recombine with the ions and emit photons. The photon energy is the sum of the kinetic energy that electrons acquired from the light field and the ionization potential of the electrons in the atom. In order to produce most energetic x rays, one has to let the electrons gain as much energy as possible from the light field in one optical cycle.

In the tunneling ionization process, the ionization rate is independent of the laser wavelength. Therefore, the saturation intensity is the same for pulses with the same duration but different wavelengths. As a result, electrons experience the same field strength at saturation intensities for pulses with different wavelengths. From Newton's laws of mechanics, we know the kinetic energy of an electron acquired in a given potential field is proportional to the square of the travel time in the field. Therefore, the electrons can gain more energy in the longer optical period field, i.e., longer-wavelength field, to generate higher-order harmonics.

Until now, the most common lasers for high-order harmonic generation are Ti sapphire, Nd:YAG, and Nd:glass lasers. Their center wavelengths are 0.8, 1.06, and 1.05 μm , respectively. Early work with different laser wavelengths (fundamental and its second harmonic) also suggested that using long-wavelength pump is favorable for reaching higher HHG photon energies [16]. But high-order harmonic generation using a pump laser with wavelength longer than 1.06 μm has rarely been explored. Using a picosecond midinfrared (3–4 μm) laser, Sheehy *et al.* produced 19th-order harmonics (~ 6 eV photon) from alkali-metal vapors [17]. Harmonic generation in the 1.2 to 1.55 μm range has been tried before at low intensity, which produced harmonics up to the 9th order (~ 8 eV photon) [18].

We performed the long-wavelength-driven experiment with a tabletop Ti:sapphire laser system [19] and an optical parametric amplifier (OPA). The generated HHG signal is measured by a transmission grating based x-ray spectrometer [20], as shown in Fig. 2. The OPA is pumped by the 25 fs, 1.2 mJ sub-kilohertz laser pulses centered at 0.8 μm , generates tunable 1.1 to 1.6- μm IR laser pulses with pulse energies ranging from 30 to 100 μJ . The OPA pulse duration is also 25 fs measured by an autocorrelator. The output of OPA is focused by an 88.3-mm lens onto the pulsed gas jet formed by a gas nozzle synchronized with the laser signal. The focal spot size is ~ 20 μm full width at half maximum (FWHM). The gas density from the pulsed jet is $\sim 1 \times 10^{18}$ atoms/cm³

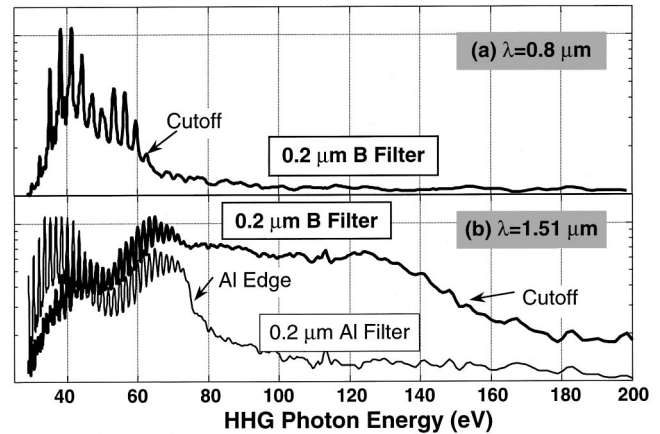


FIG. 3. HHG produced by 100- μJ , 25-fs laser pulses in argon gas. Focal point size ~ 20 μm (FWHM). Laser intensity $\sim 4 \times 10^{14}$ W/cm²; (a) 0.8- μm pump laser, cutoff at ~ 64 eV. The spectrum was measured with a 0.2- μm B filter; (b) pumped by 1.51 μm from OPA, cutoff at ~ 160 eV. The two spectra were measured with a 0.2- μm B filter (thick line) and an Al filter (thin line), respectively.

in a 200 μm interaction region. The harmonics from the gas are imaged by a focusing mirror at grazing incidence onto a chevron MCP imaging detector, which has a good sensitivity to wavelength below 140 nm. A 2000 1/mm transmission grating is employed to disperse the spectrum. Finally, the x-ray spectrum on the phosphor screen is recorded by a 16 bits cooled charge-coupled device camera. In experiments, it takes 10^5 – 10^6 shots to get a spectrum.

Figure 3 shows experimental results with argon gas. The OPA pulse energy for this experiment was measured to be 100 μJ before the interaction chamber. In the measurement, 0.2- μm Al or B filters were used to suppress the noise from the low-order harmonics. Results with the Al filter (thin line) and B filter (thick line) are both illustrated in Fig. 3(c). We can see the cutoff is at ~ 160 eV with the B filter. The harmonic peaks above 70 eV are not resolved due to the resolution of our x-ray spectrometer. This portion of radiation can be blocked by the Al filter as shown in the figure.

For comparison, we measured the HHG with an 0.8- μm laser under the same conditions. The focal spot size is kept at 20 μm and pulse energy ~ 100 μJ . The result is shown in Fig. 3(a), in which the cutoff is located at ~ 64 eV, much lower than that produced by the 1.51- μm laser. We noticed that the spacing between each adjacent harmonic peaks by the 1.51- μm driving field is about half that of the 0.8- μm pump laser, as it should be. This makes the full tunability easier for the long-wavelength driving field.

The measured cutoffs with the 0.8- and 1.51- μm pumps are both lower than the single-atom calculation results in Fig. 1. This can be accounted for by the macroscopic effect of the harmonic generation process. It is well known that the measured harmonic signal is strongly affected by phase matching. In the ionized medium the phase match length is determined by the focusing, dispersion, and intensity-dependent phase. The Rayleigh range of the focused pump beam is less than ten times of the gas medium length. Therefore, the effect of the Guoy phase shift and intensity-dependent phase

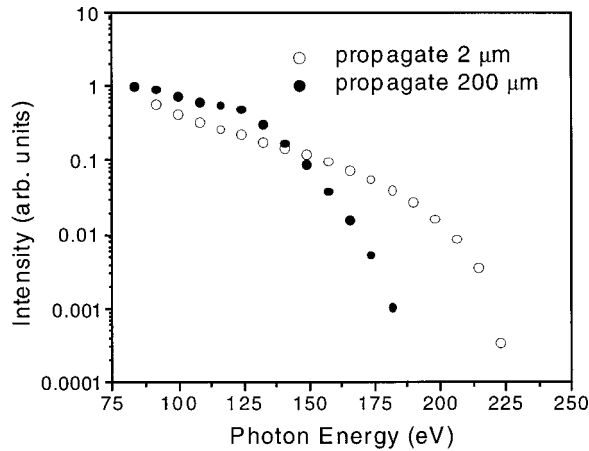


FIG. 4. Simulation of HHG intensity by 1.51- μm pump laser interacting with 2- μm and 200- μm argon gas. Laser intensity = 4×10^{14} W/cm 2 . The cutoffs of the two cases are at 225 and 180 eV, respectively.

should be significant. At our gas pressure and laser intensity, the dispersion and defocusing of plasma will definitely affect the harmonic yield. In general, these effects are stronger for higher orders, which limited the observed cutoff order.

To evaluate the macroscopic effects on the harmonic generation with long-wavelength light, we simulated the harmonic spectra using parameters that mimic our experimental conditions. First the single-atom response is calculated using the method developed by Becker, Long, and McIver [21]. The result is then put into a three-dimensional wave equation to calculate the harmonic signal from the gas. The simulation was done for argon gas with 2 μm and 200 μm medium lengths by a 1.51- μm pump. The result is shown in Fig. 4. We find that the cutoff reaches as high as 225 eV under the short-medium length (2 μm) case, where the phase mismatch is not a big problem. However, when the medium length increases to 200 μm , the cutoff dropped to ~ 180 eV, much lower than in the 2 μm case. This phenomenon has also been discussed by L'Huillier *et al.* [22]. It implies that the phase matching plays an important role under our experimental conditions. This can be improved by loose focusing the pump beam and running the experiments at low pressure or by using the hollow-core fiber technique [23].

Experiments also have been done with xenon gas. Figure 5 shows the results with xenon gas at several wavelengths. Figure 5(a) is the result produced by the fundamental 0.8- μm laser. Figures 5(b)–(d) are the results produced by the output from OPA tuned at 1.51, 1.37, and 1.22 μm , respectively. This figure also clearly illustrates the cutoff dependence on the driving-field wavelength.

At a given harmonic order, the intensity of the harmonic signal decreases with an increase of pump wavelength. We estimated the intensities of the 37th HHG peaks in Figs. 5(b)–(d). The relative intensity ratio of the spectral line for the 1.22, 1.37, and 1.51- μm pump is roughly 1:0.69:0.25. This can be accounted for by the effect of the quantum diffusion of the wave packet. As described by the semiclassical three-step model, the harmonics are generated by the recombination of the previously ionized electrons. Then the HHG

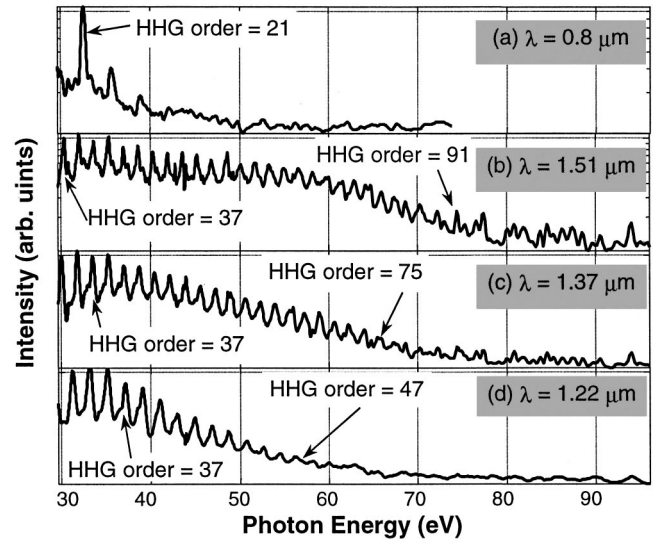


FIG. 5. HHG by 50- μJ , 25-fs laser pulses of different wavelengths in xenon gas. Focal point size ~ 20 μm (FWHM). Laser intensity $\sim 2 \times 10^{14}$ W/cm 2 . (a) 0.8 μm , cutoff at 42 eV (27th HHG); (b) 1.51 μm from OPA, cutoff at ~ 75 eV (91st HHG); (c) 1.37 μm from OPA cutoff at ~ 67 eV (77th HHG); (d) 1.22 μm from OPA, cutoff at ~ 58 eV (49th HHG). The HHG wavelength is also tuned by the driving wavelength from OPA.

field is proportional to the probability of the recombination, which is strongly affected by the overlap of the returning wave packet and the Coulomb potential well. A longer-wavelength driving field causes a longer propagation time, which leads to a bigger wave packet because of quantum diffusion. The wave packet spreads with its propagation time τ as $\tau^{3/2}$, and harmonic intensity decreases by the square of this factor [24]. Calculations based on this relationship indicate that the intensity ratio is 1:0.71:0.53 for same order HHG peaks produced by the 1.22-, 1.37-, and 1.51- μm pumps. The first ratio 1:0.71 for 1.22- and 1.37- μm pump is close to the measured value (1:0.69). However, the calculated relative intensity for the 1.51- μm pump is almost twice as large as the measured value. The discrepancy between the measured and calculated results is likely caused by both the precision of our experiments and the calculation since the analytical calculation neglects the real Coulomb potential of atoms. Compared to the measurements of harmonic efficiency and nonsequential ionization with elliptically polarized light [25], the method demonstrated here provides a powerful way to study quantum diffusion of the wave packet in the strong field.

Another advantage of using an OPA is its tunability, which consequently gives the tunability of the generated HHG emission. It is well known that high-order harmonic generation produces only odd harmonics except when the pump pulses are close to single cycle. For spectroscopic applications, it is highly desirable to tune the harmonic peak positions to hit the resonance of the matter to be studied [26]. In Fig. 5, the photon-energy range covered by the 37th harmonic of 1.22 μm and the same harmonic order of the 1.51 μm is much larger than the gap between the adjacent odd harmonic orders of either driving field. That means one can

tune the harmonic to any position in the gap. In fact, full tunability can be realized at much lower harmonic orders [18].

Assume the OPA output can be tuned between λ_1 and λ_2 . If the q th harmonic of λ_1 can be tuned to the adjacent harmonic of λ_2 , i.e., $\lambda_1/q = \lambda_2/(q+2)$, the HHG spectrum above λ_1/q will be fully tunable. Our OPA can be tuned between 1.1 and 1.6 μm , thus the above equation gives $q = 5$. Therefore, the HHG source pumped by this OPA is completely tunable from $1.1/5 = 0.22 \mu\text{m}$ up to the cutoff. This is the first demonstration of full tunability in the soft x-ray range with an OPA. Compared to the previously proposed tuning scheme with wave mixing that requires precise temporal and spatial overlap of the strong fixed-wavelength pulses and the tunable weak OPA pulses [27,28], the method demonstrated here is much simpler. It also should be noted that the wave mixing experiment so far shows only partial tuning, e.g., $<70\%$ of the gap between the adjacent orders.

In conclusion, high-order harmonic generation is studied in the 1.2–1.5- μm pump wavelength range using an ultrafast high intensity optical parametric amplifier. This type of OPA also can be used to study other nonperturbative responses of matter to the long-wavelength field. Our results show that using a long-wavelength pump is a very effective way to extend the cutoff of harmonic radiation, as predicted by the existing theories. Based on this work, we predict that ul-

trafast coherent keV x-rays can be generated by further increasing the intensity of the OPA and interacting with atoms with larger ionization potential. Even longer-wavelength driving field will also lead to further extension of harmonic cutoff, which can be done with the idler of the OPA. However, compromise must be searched between harmonic intensity and wavelength range. Our experiments show that the harmonic signal is weaker for longer-wavelength driving fields, which is consistent with the semiclassical theory. The intensity difference of the same order harmonics produced by several wavelength pumps is attributed to the effect of quantum diffusion. The harmonic radiation generated by OPA is fully tunable from vacuum ultraviolet to x ray. Just like OPA is currently significant to spectroscopy studied in the UV to IR range, the tunable x-ray source will have a big impact on applications of ultrafast coherent x ray.

The authors gratefully acknowledge support from the National Science Foundation through the STC Center for Ultrafast Optical Science. This work was also supported by the Office of Basic Energy Science, Division of Chemical Science, U.S. Department of Energy under Grant No. DE-FG02-00ER15082. We acknowledge Dr. P. Heimann, Lawrence Berkeley National Laboratory, for loaning us the x-ray spectrometer.

-
- [1] A. McPherson, G. Gibson, H. Jara, U. Johann, T. S. Luk, I. McIntyre, K. Boyer, and C. K. Rhodes, *J. Opt. Soc. Am. B* **4**, 595 (1987).
- [2] M. Ferray, A. L’Huillier, X. F. Li, L. A. Lompre, G. Mainfray, and C. Manus, *J. Phys. B* **21**, L31 (1988).
- [3] P. Salieres, A. L’Huillier, Ph. Antoine, and M. Lewenstein, *Adv. At., Mol., Opt. Phys.* **41**, 83 (1999).
- [4] T. Brabec and F. Krausz, *Rev. Mod. Phys.* **72**, 545 (2000).
- [5] Z. Chang, A. Rundquist, H. Wang, M. M. Murnane, and H. C. Kapteyn, *Phys. Rev. Lett.* **79**, 2967 (1997).
- [6] C. Spielmann *et al.*, *Science* **278**, 661 (1997).
- [7] A. Rousse, C. Rischel, and J. C. Gauthier, *Rev. Mod. Phys.* **73**, 17 (2001).
- [8] M. W. Walser, C. H. Keitel, A. Scrinzi, and T. Brabec, *Phys. Rev. Lett.* **85**, 5082 (2000).
- [9] D. B. Milosevic, S. Hu, and W. Becker, *Phys. Rev. A* **63**, 011403(R) (2000).
- [10] M. Brewczyk and K. Rzazewski, *J. Phys. B* **34**, L289 (2001).
- [11] Z. Chang, A. Rundquist, H. Wang, M. M. Murnane, and H. C. Kapteyn, *Phys. Rev. Lett.* **82**, 2006 (1999).
- [12] M. V. Ammosov, N. B. Delone, and V. P. Krainov, *Sov. Phys. JETP* **64**, 1191 (1986).
- [13] J. L. Krause, K. J. Schafer, and K. C. Kulander, *Phys. Rev. Lett.* **68**, 3535 (1992).
- [14] P. B. Corkum, *Phys. Rev. Lett.* **71**, 1999 (1993).
- [15] K. C. Kulander, K. J. Schafer, and J. L. Krause, in *Super-Intense Laser-Atom Physics*, Vol. 316 of *NATO Advanced Study Institute, Series B: Physics*, edited by B. Piraux, Anne L’Huillier, and K. Rzazewski (Plenum, New York, 1993), p. 316.
- [16] P. Balcou, C. Cornaggia, A. S. L. Gomes, L. A. Lompre, and A. L’Huillier, *J. Phys. B* **25**, 4467 (1992).
- [17] B. Sheehy, J. D. D. Martin, L. F. DiMauro, P. Agostini, K. J. Schafer, M. B. Gaarde, and K. C. Kulander, *Phys. Rev. Lett.* **83**, 5270 (1999).
- [18] M. Bellini, *Appl. Phys. B: Lasers Opt.* **70**, 773 (2000).
- [19] O. Albert, H. Wang, D. Liu, Z. Chang, and G. Mourou, *Opt. Lett.* **25**, 1125 (2000).
- [20] D. A. Mossessian, P. A. Heimann, E. Gullikson, R. K. Kaza, J. Chin, and J. Akre, *Nucl. Instrum. Methods Phys. Res. A* **347**, 244 (1994).
- [21] W. Becker, S. Long, and J. K. McIver, *Phys. Rev. A* **41**, 4112 (1990).
- [22] A. L’Huillier *et al.*, *Phys. Rev. A* **48**, R3433 (1993).
- [23] Andy Rundquist *et al.*, *Science* **280**, 1412 (1998).
- [24] M. Lewenstein, Ph. Balcou, M. Yu. Ivanov, Anne L’Huillier, and P. B. Corkum, *Phys. Rev. A* **49**, 2117 (1994).
- [25] P. Antoine, B. Carré, A. L’Huillier, and M. Lewenstein, *Phys. Rev. A* **55**, 1314 (1997).
- [26] D. Riedel, J. L. Hernandez-Pozos, R. E. Palmer, S. Baggott, K. W. Kolasinski, and J. S. Foord, *Rev. Sci. Instrum.* **72**, 1977 (2001).
- [27] M. B. Gaarde, P. Antoine, A. Persson, B. Carre, A. L’Huillier, and C. G. Wahlstrom, *J. Phys. B* **29**, L163 (1996).
- [28] H. Eichmann, S. Meyer, K. Riepl, C. Momma, and B. Welleghausen, *Phys. Rev. A* **50**, R2834 (1994).